Supplementary Information

Ultrasensitive Na^+ exchanging performance of free-standing $Fe_3O_4@Na_2Ti_3O_7$ nanosheets indicated by fluorescein†

Xuebo Cao,[a,]* Xiudong Xue,[a] Lianwen Zhu,[a] Peng Chen,[a] Yingying Song[a] and Meng Chen[b,]*
[a] Key Lab of Organic Synthesis of Jiangsu Province and Department of Chemistry, Soochow University, Suzhou, Jiangsu 215123, P. R. China.Fax:86-512-65880089;Tel:86-512-65880019;
E-mail: xbcao@suda.edu.cn
[b]Department of Chemistry, Fudan University
Shanghai 200433 (P. R. China)
E-mail: chenmeng@fudan.edu.cn

Table S1. Experimental conditions, chemical compositions, and morphologies for various samples involved in the studies

starting Materials	reaction *T* (ºC)	reaction *t* (h)	Chemical Compositions	Fe : Ti : Na (molar ratio, ICP)	morphology
TiO_2 (0.07 g) + Fe (0.015~0.02 g) +NaOH (10 g) + H_2O (25 mL)	160	48	Fe_3O_4 + $Na_2Ti_3O_7$	1 : 3.2 : 2.1	Nanosheets
TiO_2 (0.07 g) + NaOH (10 g) + H_2O (25 mL)	160	48	$Na_2Ti_3O_7$	--	Nanotubes
TiO_2 (0.07 g) + NaOH (10 g) + H_2O (25 mL)	180	48	$Na_2Ti_3O_7$	--	Nanobelts
Fe (0.015~0.02 g) + NaOH (10 g) + H_2O (25 mL)	160	48	Fe_3O_4	--	Irregular particles

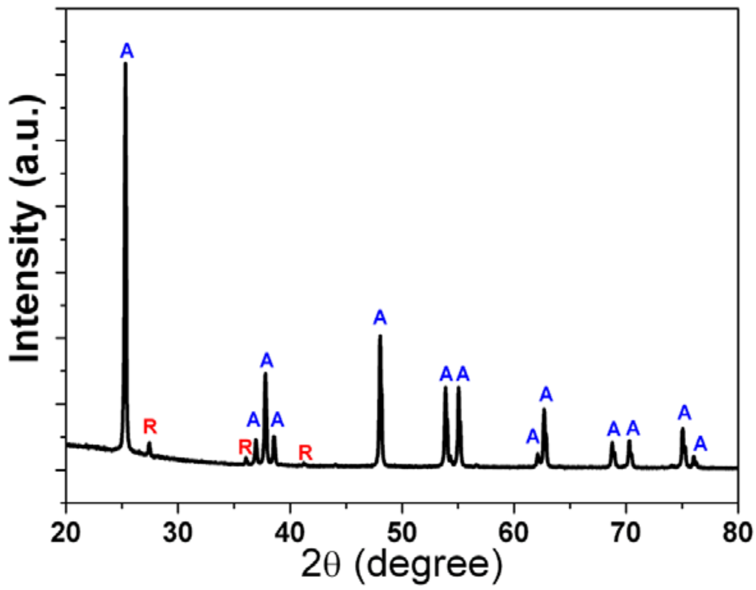

Figure S1. XRD pattern of the TiO_2 used in the synthesis, where A and R denote anatase and rutile, respectively.

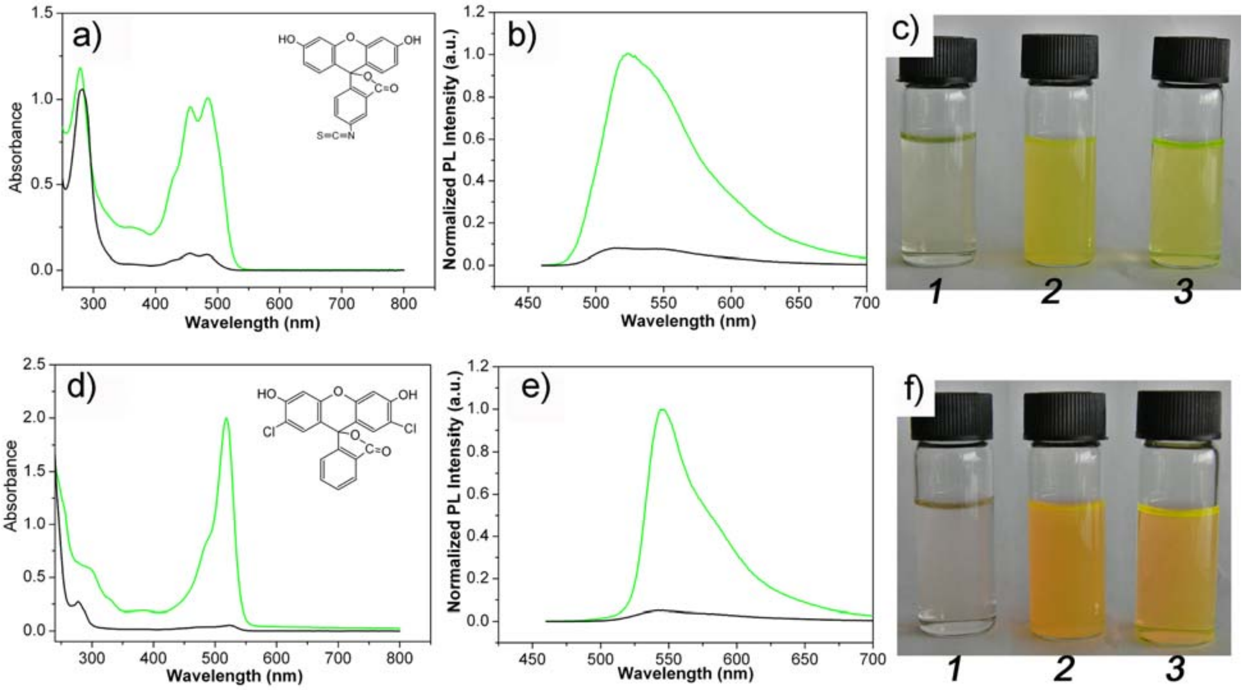

Figure S2. This figure shows the interactions of $Fe_3O_4@Na_2Ti_3O_7$ nanosheets with FITC (top) and FDC (bottom). a, d) UV-vis absorption spectra of solution **1** (black line) and **3** (green line). Insets: Structural formula of FITC and FDC. b, e) Normalized PL spectra of solution **1** (black line) and **3** (green line). Excitation wavelength: 450 nm. c, f) Photographs of the initial solution (**1**), the solution after adding $Fe_3O_4@Na_2Ti_3O_7$ nanosheets (**2**), and the solution after separating the nanosheets (**3**). The significant enhancement of absorbance and fluorescence in these FL derivates share a same mechanism as the description in FL.

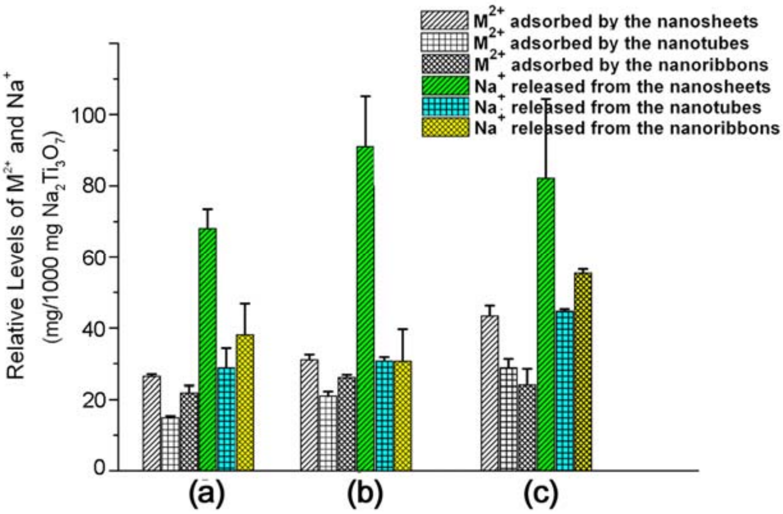

Figure S3. Ions exchange between interlayer Na^+ in various $Na_2Ti_3O_7$ nanostructures and heavy metal ions M^{2+}. A: M = Cd; B: M = Cu; C: M = Pb. In all cases, Fe_3O_4@$Na_2Ti_3O_7$ nanosheets showed the highest releasing level of Na^+ and adsorption level of M^{2+}.

The ion exchange experiments were conducted as follows: firstly, 25 mL of aqueous solution of M^{2+} (M=Cd, Cu, or Pb) with a concentration of 1.0 mmol/L were prepared. Then, 10 mg of Fe_3O_4@$Na_2Ti_3O_7$ nanosheets or $Na_2Ti_3O_7$ nanotubes or $Na_2Ti_3O_7$ nanoribbons was dispersed in the respective solutions and stirred for 24 h for sufficient exchange between interlayer Na^+ in titanates nanostructures and M^{2+} in the solution. After that, solids were separated from the solution by centrifugation at a rate of 2000 rpm and washed four times with deionized water. Both the solids and the supernatants containing Na^+ released by titanates were collected. Na^+ in the supernatants was directly analyzed by ICP-AES. To determine the amounts of M^{2+} fixed by various titanate nanostructures, the collected solids were dissolved by concentrated HNO_3. The resulting solutions were then analyzed by ICP-AES.

Table S2. The adsorption ability of per gram titanate nanostructures towards Cd^{2+}, Cu^{2+}, and Pb^{2+}

	Cd^{2+} (mg)	Cu^{2+} (mg)	Pb^{2+} (mg)
Fe_3O_4@$Na_2Ti_3O_7$ nanosheets	26.2	30.4	40.5
$Na_2Ti_3O_7$ nanotubes	14.7	20.2	30.6
$Na_2Ti_3O_7$ nanoribbons	21.3	25.4	23.8

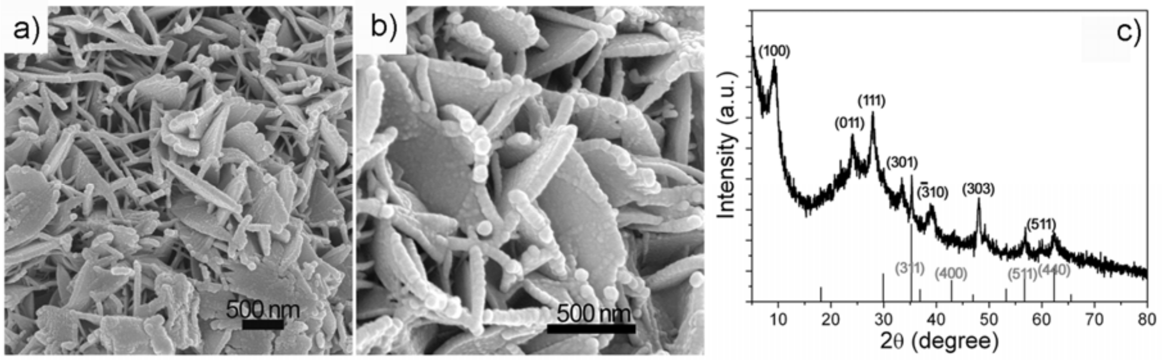

Figure S4. a, b) SEM images and c) XRD pattern of Fe_3O_4@$Na_2Ti_3O_7$ nanosheets after interactions with FL four times. The nanosheets still maintained their morphology and structure well, suggesting that they were quite stable.